



REDUCTION OF STRESS CONCENTRATION AT THE CORNER BENDS OF THE ANTI-ROLL BAR BY USING PARAMETRIC OPTIMISATION

M. Murat TOPAÇ, H. Eren ENGİNAR, N. Sefa KURALAY

Department of Mechanical Engineering
Dokuz Eylül University, 35100
Bornova, Izmir, Turkey
murat.topac@deu.edu.tr

Abstract- Stress concentration at the corner bends of an anti-roll bar that is designed for an intercity passenger bus is reduced by optimising the shape of the critical regions. In order to do this, parameters which constitute the geometry of the stress concentrated regions are determined. The effect of these parameters on stress concentration is evaluated by using Design of Experiments (DoE) approach. Possible design options and their corresponding mass and maximum equivalent stress values are obtained by using finite element analysis. The results are assessed by means of response surfaces generated by FEA software. Transition form that gives optimum stress concentration is determined.

Keywords- Anti-roll Bar, Stress Concentration, Design of Experiments Method, Parametric Optimisation, Finite Element Analysis

1. INTRODUCTION

During the vehicle service life, dynamic forces produce dynamic stresses which may cause fatigue failure of an anti-roll bar that is one of the basic parts of a suspension system used to reduce the roll tendency of the vehicle body. Recent studies showed that satisfying the static strength conditions does not mean that the mechanical part has infinite fatigue life [1]. Because of this, during the design process of a mechanical element, it is vital to take the fatigue life assessment into account. As long as the material and/or the manufacturing process have not been changed, tensile strength and therefore fatigue strength of a mechanical part cannot be altered [2]. Reducing stress concentration at the critical regions of a mechanical element is an effective alternative way to obtain a longer fatigue life [3]. On the other hand, one of the main targets to be reached in the design of vehicle suspension components is to keep the unsprung mass as small as possible with a homogenous stress distribution on the part body [4],[5]. Therefore an optimal design process of the mechanical part is inevitable.

In this study, an anti-roll bar that will be used in the front axle suspension of a 17 metric tonnes capacity passenger bus shown in Figure 1 is redesigned to minimise the stress concentration at the corner bends. In order to do this, regions that are under stress concentration during the roll motion of the vehicle body are determined by using finite element analysis. Geometric parameters which constitute the form of these regions are assigned. In the light of the results obtained from the stress analyses that were carried out for the different values of these parameters, stress and mass alteration are assessed by using Design of Experiments (DoE) approach. The effects of these

modifications on stress concentration and anti-roll bar mass are studied. Response surfaces for maximum von Mises stress and the mass of the anti-roll bar are also constructed by ANSYS® Workbench™ V11.0 commercial finite element software package. By using these results, transition form among the design candidates that gives minimum stress concentration is determined.

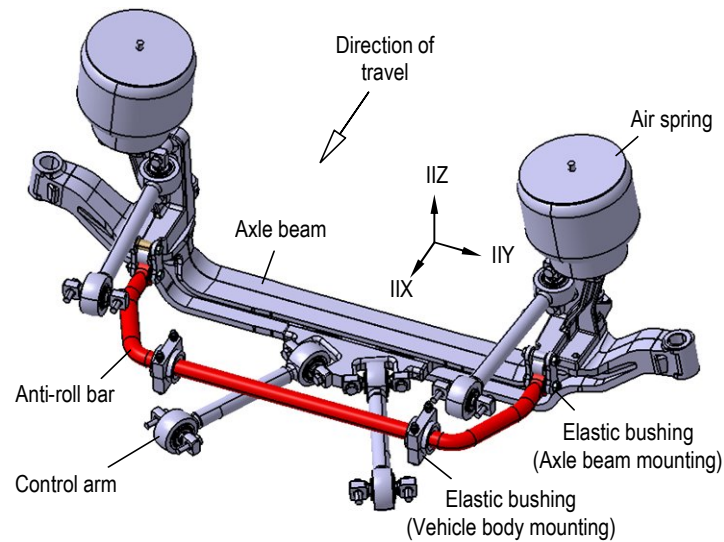


Figure 1. Front suspension of the passenger bus.

2. FINITE ELEMENT ANALYSIS OF THE ANTI-ROLL BAR

2.1. CAD and FE models

A detailed CAD model of the anti-roll bar is given in Figure 2. The anti-roll bar is mounted to the vehicle body (H and H') and axle beam (F and F') via elastic bushings. The stress analyses are performed via ANSYS® Workbench™ V11.0 commercial finite element software. The FE model formed for the analysis is composed of 74,413 elements and 132,741 nodes. To build this model, CAD model of the anti-roll bar is meshed using SOLID187, a higher order three dimensional solid element, which has quadratic displacement behaviour and is well suited to model irregular meshes. The element is defined by 10 nodes having three translational DOF at each node [6], [7]. Each arm mounting of this model consists of three elements. The details of the FE model are shown in Figure 3. Here, elastic bushing (2) and the connection bolt (3) can rotate freely around their own axes. They also have a limited sliding freedom along the Y axis. The friction is neglected. In the FE model, it was assumed that elastic bushings are made of rubber. In literature, modulus of elasticity is given as $E_{\max} = 0.1$ (GPa) and Poisson's ratio $\nu \approx 0.5$ for this material [8], [9]. For the limited deformation of the bushings, behaviour of the material was assumed as linear isotropic. Anti-roll bar will be manufactured from 50CrV4 (51CrV4) spring steel that is suitable for highly stressed spring design. Basic mechanical properties of this material after quenching are given in Table 1 [10].

Reduction of Stress Concentration at the Corner Bends of the Anti-Roll Bar

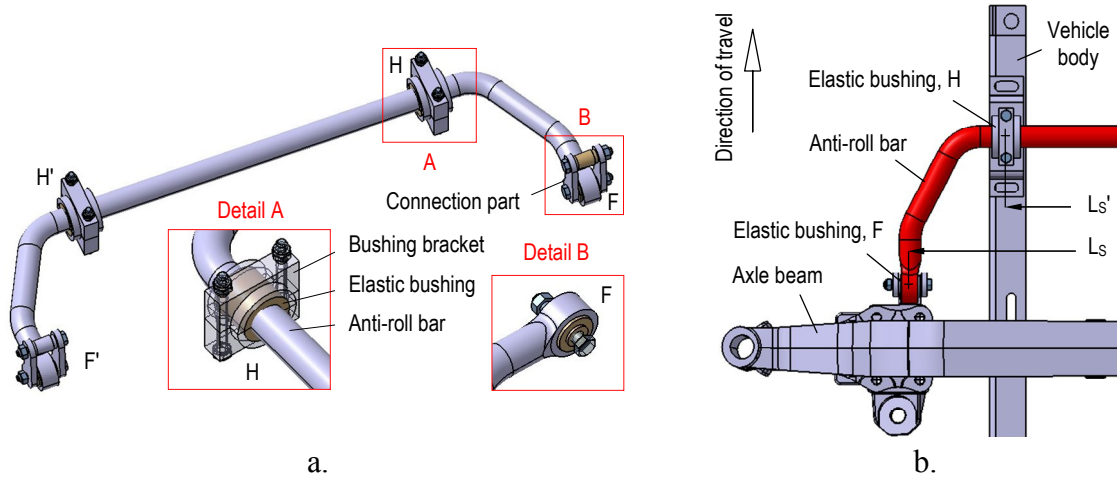


Figure 2. a. Elastic bushings of the anti-roll bar, b. Position of bushing points.

Table 1. Mechanical properties of the 50CrV4 (51CrV4) steel [10].

Standard	EN 10 083
Material number	1.8159
Modulus of elasticity, E (GPa)	200
Poisson's ratio, ν (-)	0.3
Yield strength (min.), S_v (MPa)	800
Ultimate strength (min.), S_{ut} (MPa)	1000

2.2. Determination of loading conditions

The average lateral acceleration of the vehicle body during the service predicted by the manufacturer is about $a_q=3(m/s^2)$. In the previous work of Topaç and Kuralay, body roll characteristic of the passenger bus was determined by using equivalent roll stiffness approach and validated via a full dynamic simulation of the vehicle. According to the results of this work, the roll angle of the vehicle body was calculated as $\varphi \approx 1.71(^{\circ})$ for $a_q=3(m/s^2)$. The roll simulation of the passenger bus is shown in Figure 4 where, SP' is the center of mass, M' roll center, a_q the centrifugal acceleration and φ the roll angle of the vehicle body [11]. The schematic representation of elastic deformation of the anti-roll bar arms during cornering manoeuvre of the vehicle is given in Figure 5 where c_{sv} (N.mm/ $^{\circ}$) is the torsion stiffness. By using this geometry, twist angle θ can be calculated as $\theta=3.17(^{\circ})$ with the equation;

$$\text{tg}\theta = \frac{S_{sv}}{2a} \text{tg}\varphi \quad (1)$$

Hence, the deformation of the anti-roll bar arms at F or F' bushings along the Z axis is calculated as $z_1 = z_2 = 17$ (mm) by using the expression,

$$z_1 = a \cdot \text{tg}\theta \quad (2)$$

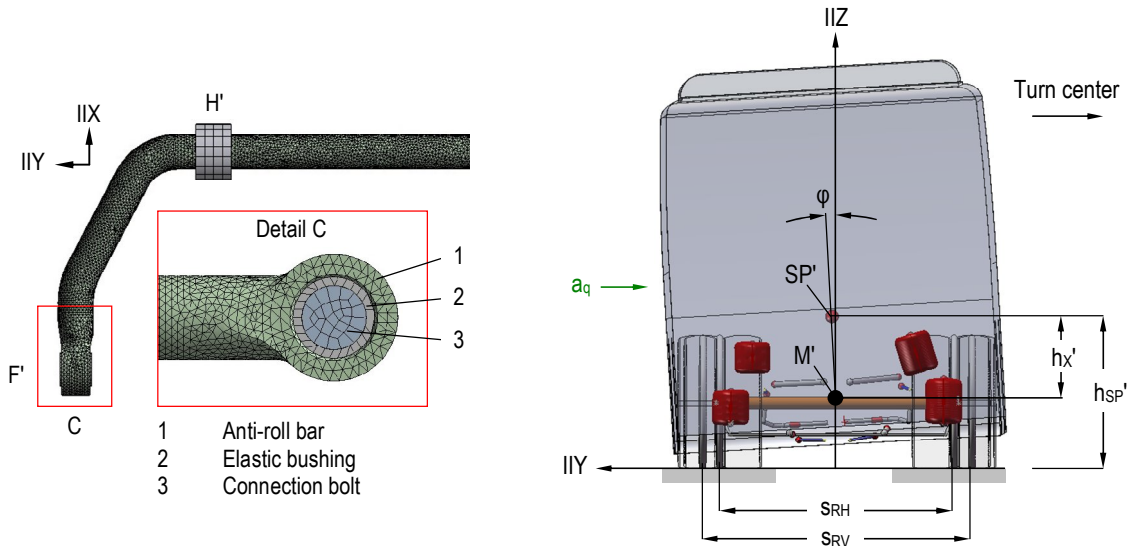


Figure 3. FE model of the anti-roll bar. Figure 4. Roll simulation of the passenger bus

2.3. Finite element analysis

The stress analysis of the anti-roll bar was carried out via ANSYS® Workbench™ V11.0 commercial finite element software. For the analysis, the displacement $z_1 = z_2 = 17$ (mm) was applied on arm bearings F and F' at the opposite directions. The elastic deformation distribution of the anti-roll bar body is given in Figure 6.

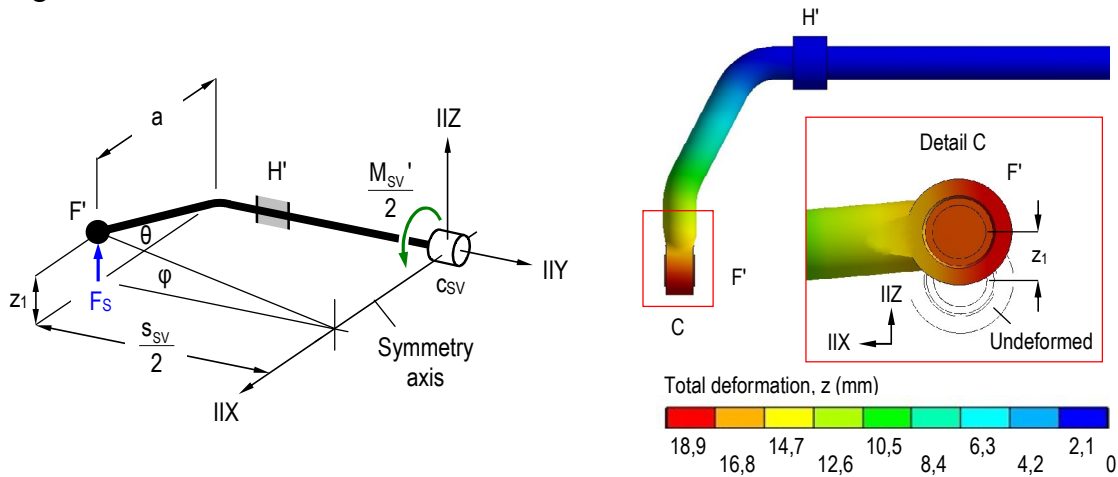


Figure 5. Elastic deformation of the anti-roll bar due to the roll angle.

Figure 6. Deformation of the anti-roll bar in Z axis

The results of the stress analysis are also shown in Figure 7. According to these results, equivalent von Mises stress between the bearings H and H' is about $\sigma = 300$ (MPa). The maximum equivalent stress is determined at the section E-E as $\sigma_{max} \approx 363.3$ (MPa); 45.4 % of the yielding point of material. The minimum value of factor of safety

for static loading is also calculated as $n = 2.2$. FE analysis that simulates the cornering manoeuvre of the passenger bus showed that there are stress concentrated regions at the corner bends of the anti-roll bar. It is also known from literature that an anti-roll bar may fail at these regions because of mechanical fatigue caused by stress concentration [12], [13]. An example of this type of fatigue failure is given in Figure 8 [12]. Therefore, application of the form optimisation process to minimise the stress concentration at these regions of the anti-roll bar that is subjected to dynamic loading during the service life of the vehicle is indispensable.

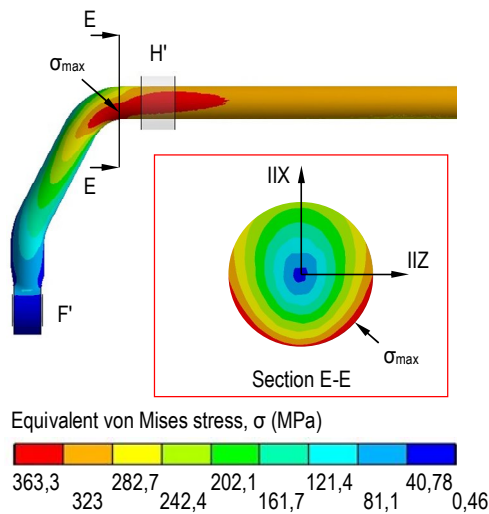


Figure 7. Stress analysis of the anti-roll bar.



Figure 8. Fatigue failure of an anti-roll bar due to the stress concentration [12].

3. PARAMETRIC OPTIMISATION

3.1. Determination of geometric parameters

Dimensions of the anti-roll bar are given in Figure 9. In order to reduce the stress concentration and accordingly, the stress concentration factor K_t at the determined critical regions, design enhancement of anti-roll bar corner bends has been proposed. This change has been found to depend on two geometric parameters. To what extent the modification in these parameters alter the stress concentration and mass has also been examined. The geometric parameters determined at the critical regions are,

- Transition radius, R
- Transition length, L_2

According to Figure 5 and Figure 9, the maximum stress at the critical corner bend regions of the anti-roll bar can be expressed as;

$$\sigma_{\max} \approx \frac{32}{\pi \cdot d^3} \cdot \left(\frac{c_{SV}}{b_g} \cdot \frac{2 \cdot \theta}{z_{1,2} \cdot a} \right) \cdot z_{1,2} \cdot L_{10} \cdot K_M \quad (3)$$

Here b_g is the bearing factor for elastic bushings. K_M is a factor that can be expressed as;

$$K_M = f(p; q) \quad (4)$$

where $p = R/L_{10}$ and $q = L_9/L_{10}$. The effect of these two geometric parameters on K_M can be obtained from literature [14], [15], [16]. Decreasing both p and q reduces the K_M value. On the other hand, reducing L_{10} decreases σ_{\max} . In other words, it is expected that increasing the dimension L_2 reduces the maximum stress at the critical regions. According to equation (3), position of bushing mountings H and H' does not have any remarkable effects on stress concentration at these points.

The limit values used for geometric parameters are given in Table 2. In addition, according to the design restriction predicted by the manufacturer, mass increase of anti-roll bar mass should not be higher than $\Delta m_s = 1$ (kg). The initial value of m_s is 28.09 (kg).

Table 2. Limit values for design parameters.

Parameter	Initial value	Design limits
Transition radius R (mm)	75	$75 < R \leq 135$
Transition length L_2 (mm)	465	$465 < L_2 \leq 535$

3.2. Parametric optimisation

In order to optimise the anti-roll bar shape and obtain the minimum value of stress concentration at the critical regions determined via the primary stress analysis, DesignXplorer™ module of ANSYS® Workbench™ V11.0 commercial finite element software was utilised. To build the solid model, SolidWorks® commercial software was also used. To carry out the optimisation process, firstly input and output parameters were determined. Then DesignXplorer™ module was started and Design of Experiments (DoE) method was chosen. Nine automatic design points were generated for two input parameters; R and L_2 by the software package in pursuance of the workflow of DesignXplorer™ that is given in Figure 10. Stress analyses that correspond to these points were carried out. By using the results of these analyses, 3-D response surfaces for maximum von Mises stress and anti-roll bar mass were also generated by the FEA software. At the following step, in the light of the design targets and limitations, “Goal Driven Optimisation (GDO)” approach was utilised to predict the best combination of the chosen parameters by using these results. Targeted design point that corresponds to optimal geometry of the anti-roll bar was estimated.

4. RESULTS AND DISCUSSION

Maximum von Mises stress, σ_{\max} and anti-roll bar mass, m_s values calculated for the design points specified by parametric optimisation software are given in Table 3. By using these results, response surfaces for σ_{\max} and m_s as functions of R and L_2 are also generated by FEA software that are given in Figure 11 and Figure 12. The effect of the

transition length L_2 on stress concentration and mass for selected values of the transition radius R is seen in Figure 13 and Figure 14. Analyses showed that, reduction of stress concentration is possible by increasing the geometric parameter L_2 from 465 to 535 (mm). The calculated decrease is 8.6% for $R= 75$ (mm) and 7.7% for $R= 135$ (mm) which are the two limit values for the transition radius.

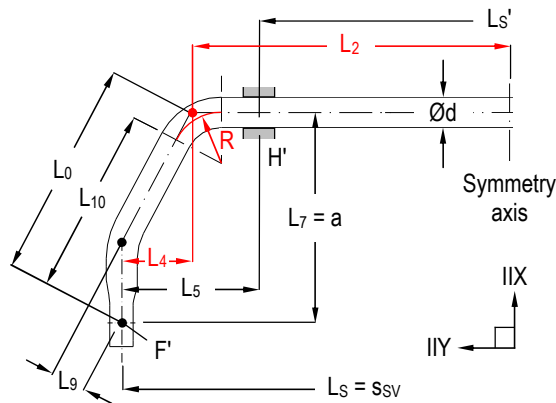


Figure 9. Basic dimensions of the anti-roll bar.

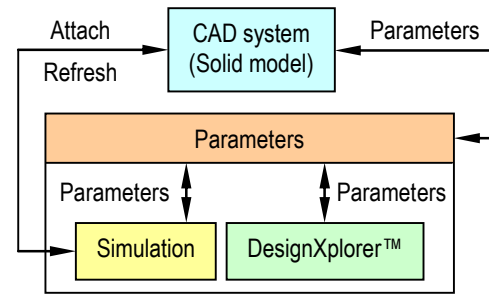


Figure 10. General application workflow of DesignXplorer™ (according to [17]).

Table 3. Calculated maximum stress, σ_{\max} and mass, m_s values for specified design points.

Parameter	Design point 1	Design point 2	Design point 3	Design point 4	Design point 5	Design point 6	Design point 7	Design point 8	Design point 9
Transition radius, R (mm)	105	75	135	105	105	75	135	75	135
Transition length, L_2 (mm)	500	500	500	465	535	465	465	535	535
Maximum stress, σ_{\max} (MPa)	338.7	342.32	344.02	358.77	328.99	365.57	362.63	329.82	335.22
Mass, m_s (kg)	28.435	28.609	28.261	27.982	28.917	28.093	27.869	29.19	28.644

It was also determined that higher L_2 value causes a mass increase of about 3.9% for $R= 75$ (mm) and 2.8% for $R= 135$ (mm). The effect of the transition radius R on stress concentration and mass is also seen in Figure 15 and Figure 16. The analyses pointed out that increasing the transition radius affects as a stress riser, over an optimum R value. It was also determined that larger corner bend radius reduces anti-roll bar mass to a certain extent. The calculated decrease is 1.9% for $L_2= 535$ (mm) and 0.8% for $L_2= 465$ (mm).

The optimal values of the chosen parameters are estimated via Design of Experiments method as $R= 86.49$ (mm) and $L_2= 534.2$ (mm). To validate this result, a CAD model of the anti-roll bar that corresponds to these new values was prepared and finite element analysis was also applied to this model. The results of this analysis showed that the difference between the predicted and calculated values is 0.34% for maximum von Mises stress. The comparison of the DoE prediction and finite element analysis is given in Table 4. Since increasing L_2 decreases the maximum stress, FE

analyses of the anti-roll bar form of $L_2= 565$ (mm) which corresponds to U-shape were also carried out for different R values. The results of these analyses are given in Figure 17. Minimum σ_{\max} value was obtained as 321.84 (MPa) for $R= 83.3$ (mm) as seen in Figure 18. However, mass of this design was calculated as $m_S= 29.6$ (kg) that is higher than the design limitation. On the other hand, difference of maximum stress obtained from these two designs is only 1.21%. Because of this, dimensions that are given in Table 4 can be assumed as optimal values. The total decrease of the maximum stress σ_{\max} at the critical regions for this design is calculated ca. 11% with a mass increase of 3.5%. The shape of the anti-roll bar corner bends that provides optimum stress concentration for determined design limits is given in Figure 19.

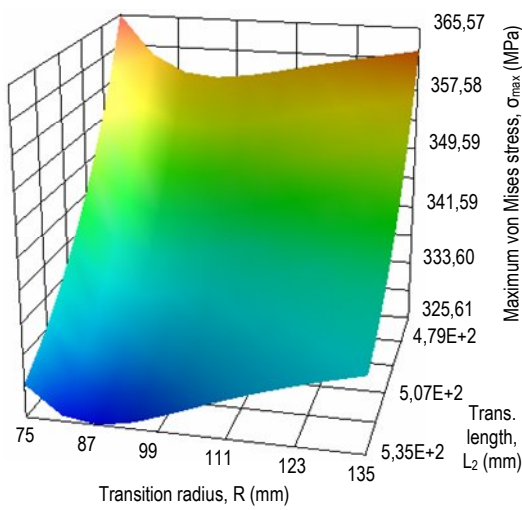


Figure 11. Response surface for maximum stress.

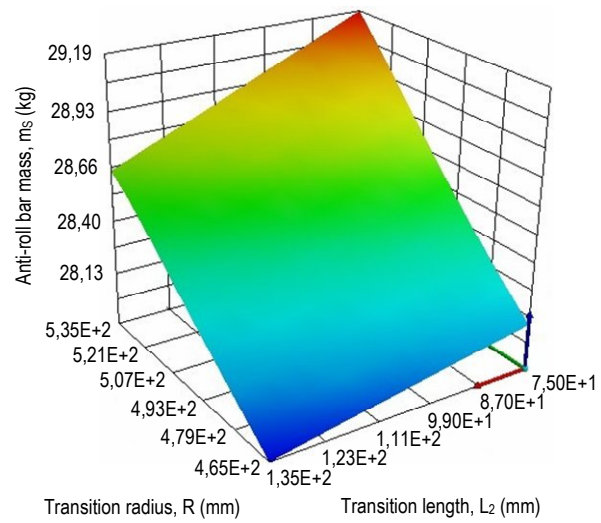


Figure 12. Response surface for anti-roll bar mass.

Table 4. Maximum stress and mass values for optimal design point.

Parameter	DoE prediction	FE analysis
Transition radius, R (mm)	86.49	86.49
Transition length, L_2 (mm)	534.21	534.21
Maximum stress, σ_{\max} (MPa)	326.9	325.78
Mass, m_S (kg)	29.073	29.075

5. CONCLUSIONS

An anti-roll bar that will be used in the front axle suspension of a passenger bus is redesigned to minimise the stress concentration at the corner bends for given structural limits. For this purpose, the effects of two design parameters; the transition length L_2 and the transition radius R that constitute the geometry of the critical regions were studied.

Reduction of Stress Concentration at the Corner Bends of the Anti-Roll Bar

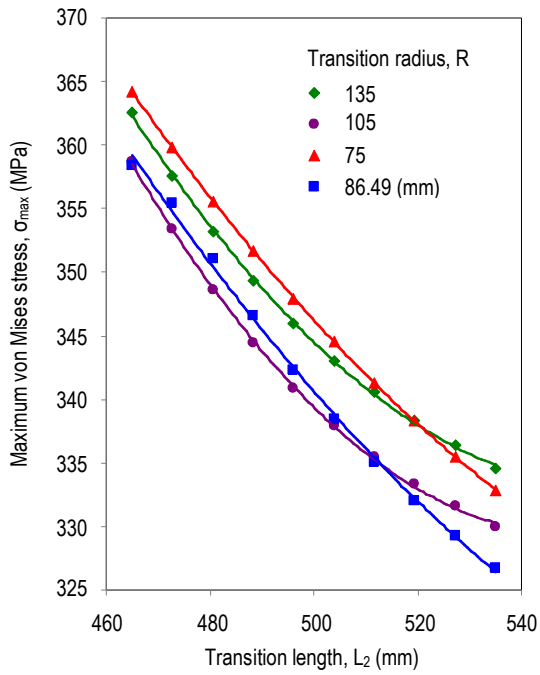


Figure 13. Effect of the increase of transition length L_2 on stress concentration.

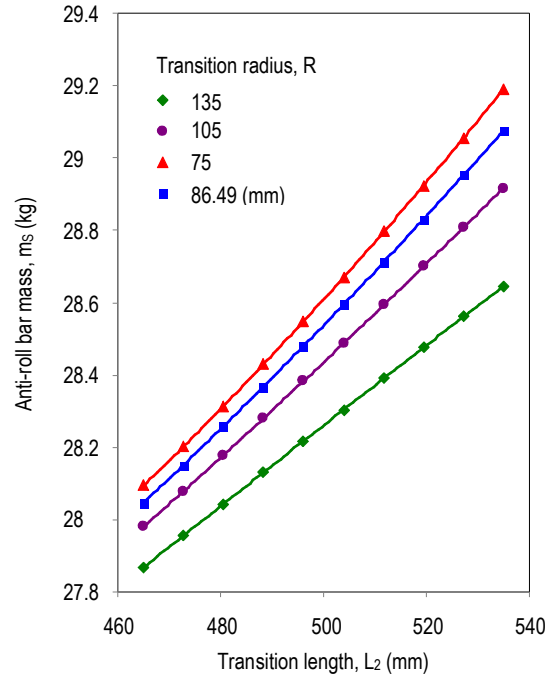


Figure 14. Effect of the increase of transition length L_2 on anti-roll bar mass.

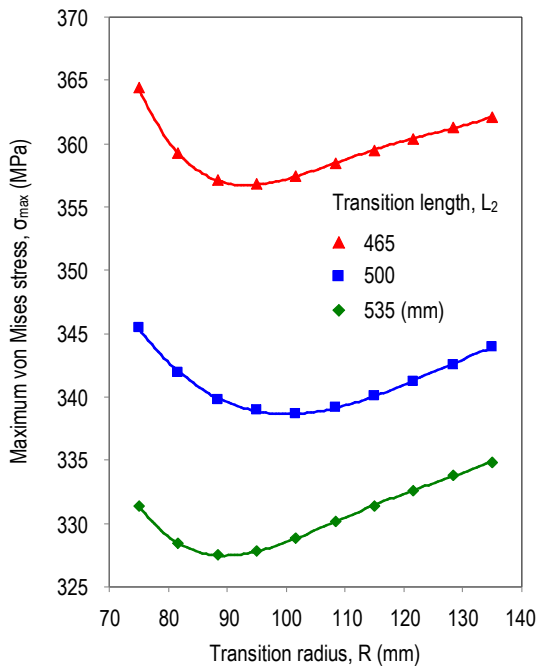


Figure 15. Effect of the increase of transition radius R on stress concentration.

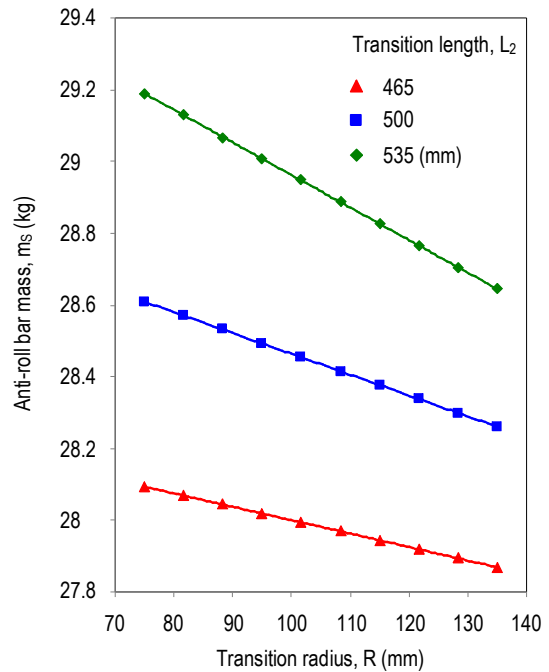


Figure 16. Effect of the increase of transition radius R on anti-roll bar mass.

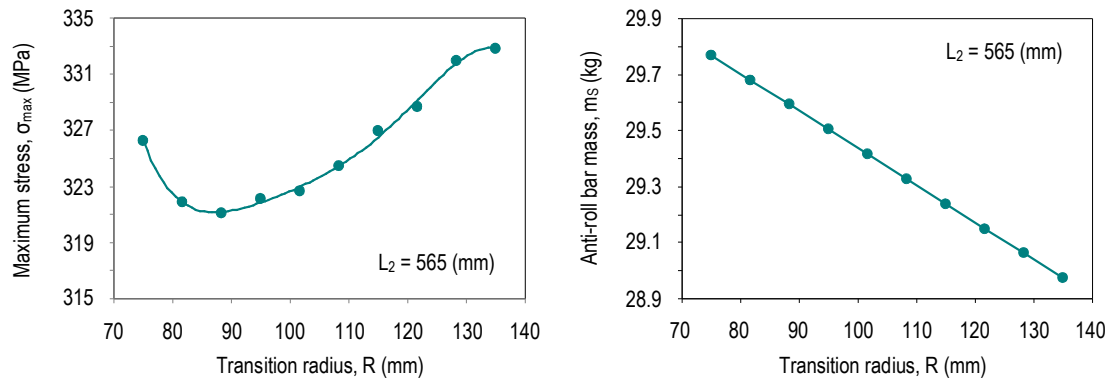


Figure 17. Maximum stress and mass values for $L_2 = 565$ (mm).

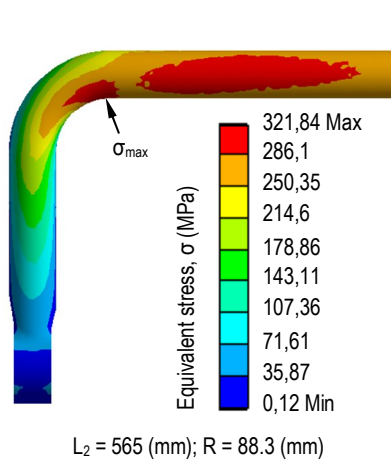


Figure 18. U-shape giving minimum stress concentration.

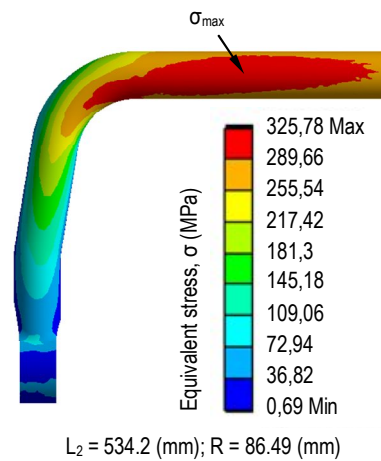


Figure 19. Optimal corner bend geometry.

The parametric optimisation was applied via ANSYS[®] Workbench[™] V11.0 commercial finite element software by using Design of Experiments (DoE) approach. FE analyses showed that it is possible to decrease the maximum stress σ_{max} at the critical regions ca. 11% with a mass increase of 3.5%. The results obtained can be summarised as follows:

- An increase of the transition length L_2 decreases the equivalent von Mises stress at the corner bends, however raises the anti-roll bar mass.
- Increasing the transition radius R raises the equivalent stress and also the notch effect at the critical regions over an optimum R value.
- Increasing the transition radius R also decreases the anti-roll bar mass.

Similar studies can be applied to the automobile anti-roll bars which have more complex shapes. By this way the optimal geometry can be determined with the lowest mass increase.

6. REFERENCES

1. Topaç, M.M.; Günal, H.; Kuralay, N.S. Fatigue failure prediction of a rear axle housing prototype by using finite element analysis. *Engineering Failure Analysis* 16(5): 1474-1482. 2009.
2. Shigley, J.E. and Mischke, C. *Mechanical Engineering Design*. New York: McGraw-Hill, Inc. 1989
3. Schijve, J. *Fatigue of Structures and Materials*, Dordrecht, Netherlands: Kluwer Academic Publishers. 2001.
4. Topaç, M.M.; Günal, H.; Kuralay, N.S. Enhancement of fatigue life of a heavy commercial vehicle rear axle housing under cyclic vertical loading by using finite element analysis. *Engineer and Machinery* 51(601): 10-20. 2010. (In Turkish with an abstract in English)
5. Jazar, R.N. *Vehicle Dynamics; Theory and Application*. New York: Springer Science+Business Media, LLC. 2008.
6. ANSYS Theory Reference. ANSYS Release 10.0, ANSYS, Inc. 2005.
7. Senalp, A.Z.; Kayabasi, O.; Kurtaran, H. Static, dynamic and fatigue behavior of newly designed stem shapes for hip prosthesis using finite element analysis. *Materials & Design* 28(5): 1577-1583. 2007
8. Ashby, M.F. and Jones, D.R.H. *Engineering Materials, an Introduction to their Properties and Applications*, Oxford: Pergamon Press. 1980.
9. Rinde, J.A. Poisson's ratio for rigid plastic foams. *Journal of Applied Polymer Science* 14(8): 1913-1926. 1970.
10. Yüksel, M. *Malzeme Bilimleri Serisi-Cilt 1: Malzeme Bilgisi*, Ankara: TMMOB Makina Mühendisleri Odası. Yayın No: MMO/2003/271/2. 2003. (In Turkish)
11. Topaç, M.M.; Kuralay, N.S. Computer aided design of an anti-roll bar for a passenger bus. *Engineer and Machinery* 50(594): 14-24. 2009. (In Turkish with an abstract in English)
12. Bayrakceken, A.; Tasgetiren, S.; Aslantas, K. Fracture of an anti-roll bar. *Engineering Failure Analysis* 13(5): 732-738. 2006.
13. Cerit M, Nart E, Genel K. Investigation into effect of rubber bushing on stress distribution and fatigue behaviour of anti-roll bar. *Engineering Failure Analysis* 17(5): 1019-1027. 2010.
14. v. Estorff, H.E. *Technische Daten Fahrzeugfedern Teil 3: Stabilisatoren, Eine Veröffentlichung der Abteilung "Forschung und Entwicklung" der Stahlwerke Brüninghaus GmbH. Werdohl (Westfalen): Stahlwerke Brüninghaus GmbH, Ausgabe September 1969. (In German)*
15. Reimpell, J. *Fahrwerktechnik Bd. 2. Würzburg: Vogel-Verlag. 1973. (In German)*
16. Kuralay, N.S. *Motorlu Taşıtlar; Temel ve Tasarım Esasları, Yapı Elemanları, Cilt 1; Tahrik ve Sürüş Sistemleri*. İzmir: TMMOB Makina Mühendisleri Odası. Yayın No: MMO/2008/484. 2008. (In Turkish)
17. Çelik, H.K.; Uçar, M.; Cengiz, A. Parametric design, stress analysis and optimization of the housing in gear pumps. *Engineer and Machinery* 49 (576): 15-24. 2008. (In Turkish with an abstract in English)